ScienceDirect

Maritime Transport Research
Volume 5, December 2023, 100100

Optimal planning of an urban ferry service operated with zero emission technology

Kenneth Løvold Rødseth [a], Kjetil Fagerholt [b], Stef Proost [c]

[a] Institute of Transport Economics – Norwegian Centre for Transport Research, Oslo, Norway
[b] Department of Industrial Economics and Technology Management, Norwegian University of Science and Technology, Trondheim, Norway
[c] Department of Economics, KU Leuven, Leuven, Belgium

Received 16 July 2023, Revised 14 September 2023, Accepted 2 October 2023, Available online 6 October 2023, Version of Record 6 October 2023.

https://doi.org/10.1016/j.martra.2023.100100
Get rights and content

Highlights

- Technical and economic feasibilities of an urban *battery-powered* passenger ferry service.
- Mixed-Integer Programming problem for fleet, frequency and speed selection.
- Application to an existing urban ferry service in Oslo, Norway.
- Zero emission technologies can pass the cost-benefit test.

- Substantial cost reductions from altering the current ferry route.

Abstract

While passenger-only ferries can be an effective instrument in mitigating road congestion in urban areas, they are among the most polluting modes of transportation. This paper studies technical and economic feasibilities of a *battery-powered* high-speed ferry service in Oslo, Norway. An urban *ferry planner problem* that minimizes ferry operator and passenger costs and external costs of road transport subject to *strategic* (fleet selection and infrastructure location), *tactical* (service frequency) and *operational* (vessel speed) decisions is proposed. While the results show that zero emission technologies can pass the cost-benefit test for a short-range service, competitiveness hinges on energy costs and capacities and on the performance of the existing service. Counterfactual scenarios show substantial cost reductions from altering the current ferry route. Anticipated increase in external costs of road transport from closing the ferry service is also much smaller than the system costs of maintaining the urban ferry connection.

Previous

Next

Keywords

Climate policy; High-speed ferry; Mixed-Integer Programming; Marine battery; Transport policy

1. Introduction

The urban transport market is characterized by many externalities. Among the costliest is road congestion during peak hours (Wangsnesset al., 2020). Increased traffic load has created a call for passenger vessel services in urban areas (Kamenand Barry,2011) to address road congestion.

Norway is an example of a county with several high-speed ferry connections in operation in urban areas, aiming to save passenger travel time and discomfort. Whilst on the one hand alleviating road congestion, high-speed ferries are considered among the dirtiest modes of transportation (Eideetal., 2018). Frostand Brooks(2021) note that sustainable urban ferry services must meet zero emission targets set by the International Maritime Organization (IMO). This aim is the focal point of the current study.

Ambitious climate policies have made Norway a front-runner in the diffusion of low and zero emission technologies for cars (Wangsnesset al., 2020). In 2021, the Norwegian Government launched its Climate Plan 2021–2030 to continue the path to sustainable transport. It aims is to halve domestic maritime transport emissions by 2030, relative to 2005 emissions. The plan includes low and zero emission requirements for ferries from 2023 and high-speed ferries from 2025 and a carbon tax of 2 000 NOK per ton by 2030. The Norwegian decarbonization program can have important spillovers to the rest of the world.

There is a vast potential for diffusion of zero emission technologies for existing conventional (slow-going) ferry connections at relatively modest abatement costs. Currently, 21.5 percent of the approximately 230 existing connections in Norway are electrified.[1]

High-speed ferries constitute an important element of Norway's coastal transport system, and there are about 100 services currently in operation. They are characterized by high energy consumption, and a recent feasibility study (Sundvoretal., 2021) show that the potential for electrification of high-speed ferries in Norway is limited. Analyzing high-speed ferry connections in Florø and Stavanger, Havreetal.(2022) estimate abatement costs of adopting battery-powered high-speed ferries to range between 3 000 and 18 000 NOK per ton of CO_2. This is substantially higher than the Norwegian Government's estimate of the social cost of carbon of 2 000 NOK per ton by 2030.

Diffusion of zero emission technologies for high-speed ferries has been modest compared to slow-going ferries: The initiative, Transport: Advanced and Modular (TrAM) launched the world's first electrical high-speed ferry in Stavanger, Norway, in September 2022. Zero emission high-speed vessels are currently also being considered for other services; cf. Sundvoretal.(2021). This paper analyzes technical and economic feasibilities of battery-powered high-speed ferries for short-range urban commuter services.

The aim of this paper is to study *optimal planning* of a high-speed ferry transport service for an existing connection subject to zero emission vessel requirements. An *urban ferry planner problem* that minimizes ferry operator and passenger costs and external costs of road transport subject to *strategic* (fleet selection and infrastructure location), *tactical* (service frequency) and *operational* (vessel speed) decisions is proposed. As the current uptake of zero emission technology mainly concerns battery-electric propulsion (Sundvoretal., 2021) the analysis is limited to marine batteries and rules out sustainable e-fuels. The model is demonstrated for a case study in Norway's capital Oslo.

This paper provides both methodological and empirical contributions to the literature. First, it adds to the scarce literature on optimal planning of high-speed passenger ferry connections subject to zero emission technology, being the first study to consider the role of high-speed passenger ferries in the urban transport market. Second, the paper evaluates technical and economic feasibilities of battery-powered vessels for a short commuter service, considering a wide range of cost drivers and mitigation options.

The current paper draws on a novel planning problem for zero emission high-speed ferries by Havreetal.(2022) but extends their contribution in several ways. Among others, external costs of road traffic and costs from congestion (i.e., crowding) onboard the ferry are incorporated into the optimization model as these are the raison d'être of most urban ferries. Second, the analysis goes beyond simply replacing an existing diesel ferry by reoptimizing the ferry route and the frequency. This is important as a shorter ferry route may be optimal to mitigate range disadvantages of battery-powered vessels, even if this comes at the expense of passenger discomfort and increased road congestion.

In contrast to Havreetal.(2022) study, our case study shows that zero emission technologies can pass the cost-benefit test for a short-range service, but that competitiveness hinges on energy costs and capacities and on the performance of the existing service. In contrast to previous papers on optimal planning of high-speed ferry services we also consider the role of route planning with the diffusion of zero emission technologies: Counterfactual scenarios show substantial cost reductions from altering the current ferry route by reducing the energy consumption required for operating the high-speed ferry service. Moreover, the system costs of the ferry service substantially outweigh the anticipated increase in external costs of additional road transport following the closing of the ferry service.

This paper is organized as follows. Section 2 sets the scene by discussing zero emission transport technologies and urban public transport and by reviewing related literature. Section 3 presents a Mixed-Integer Programming (MIP) problem for an urban high-speed ferry connection, while Section 4 reviews the parameters used for implementation. Section 5 presents the computational results while Section 6 summarizes main findings and offers managerial and policy recommendations.

2. Background and literature review

This section motivates the urban planner problem and provides a literature review.

2.1. The urban public transport market

Herein, an urban planner problem is developed to study optimal policies for ferries as a public transport service. The situation considered is *second best* where the public transit planner oversees frequency setting for the connection in question, but where fare and road toll policies are outside the decision domain of the planner. This is tailored to the Norwegian case, where public transit is provided by regional governments, but fares are largely based on (sluggish) zonal pricing. Road tolls are under the jurisdiction of city officials and thus not part of the decision domain of public transit planners.

The model developed in this paper is motivated by the literature on public transport economics. A review of relevant studies can be found in Hörcher and Tirachini (2021). Frequency setting for public transport requires attention to the Mohring-effect (Mohring, 1972) that trades off operator and waiting time costs, as well as discomfort from crowding (De Palma et al., 2015). In situations where competing modes such as the private car are not priced at social marginal costs, external costs of transport caused by diversion to or from public ferry transport is also an important consideration when determining optimal frequency. Section 3 characterizes an urban ferry transport planning model that encompasses all these considerations to identify socially optimal frequency and routing of a battery-powered vessel service.

To better convey the aims and scope of the subsequent modeling in a simple and transparent way, we provide a motivating graphical illustration. High-speed ferries usually serve to alleviate road congestion problems between suburbs and a big city. In Fig. 1, we illustrate this problem graphically for a given number of commuters N that want to access the city center from a given suburb. Commuters have a choice between the ferry and the car and choose the mode with the lowest private generalized cost, comprising monetary costs such as fares and time costs of road transport or ferry transit and waiting. Car users are measured from left to right and the high-speed ferry users from right to left in Fig. 1. Every point on the x-axis represents a distribution of the N commuters between the two modes.

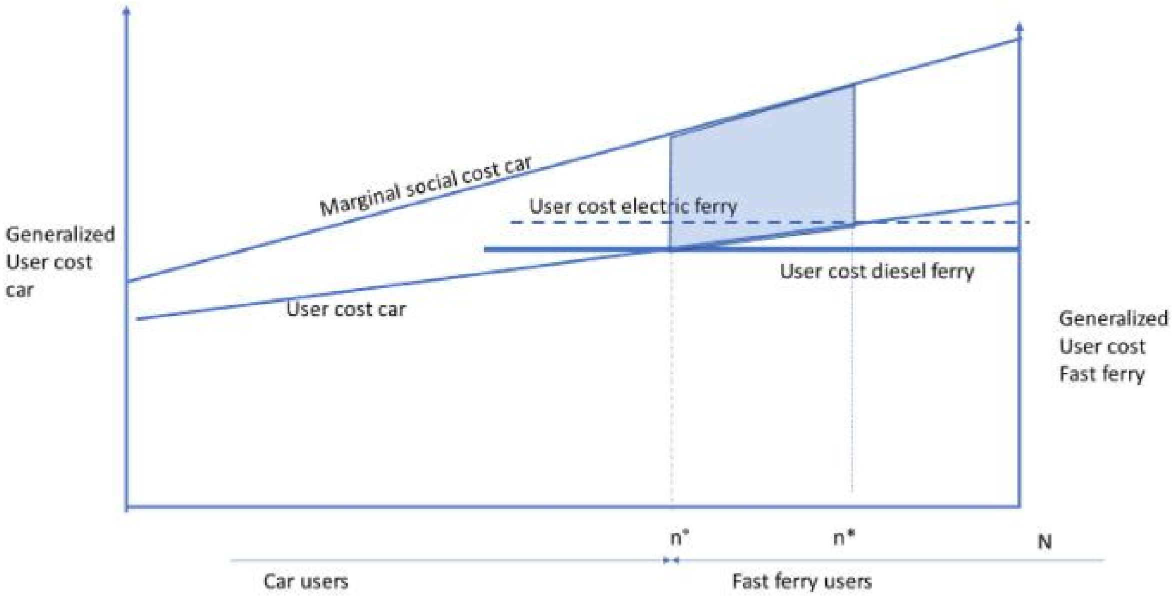

Fig. 1. Graphical illustration of the urban transport equilibrium.

As the road capacity is given, loading more cars on the road increases the average time costs, which explains the increasing average car user cost in Fig. 1. The marginal social cost of car use includes the external congestion cost and has a higher slope than the user costs because every additional road user increases the time costs for all existing users. In contrast, the user cost for a diesel ferry is taken as constant in the illustration because crowding is assumed compensated by higher frequency and ferry capacity. With a diesel ferry, there will be $n°$ car users and $(N\text{-}n°)$ ferry users in the initial transport equilibrium (when road users do not carry the full social cost of driving).

Consider now the electrification of the high-speed ferry to reduce greenhouse gases and other emissions. This will involve fixed costs (e.g., recharging installations) related to adoption of a new energy system. Electrification can also affect the user cost for the ferry service: Due to the range consideration, added charging time and corresponding cost increases of operating the battery-powered vessels service speeds may decrease and frequencies may be reduced. This means that the generalized user cost of the battery-powered ferry may be higher than that of the diesel ferry. In Fig. 1, this implies an upward shift of the ferry user cost which results in a decrease of the number of ferry users from $N\text{-}n°$ to $N\text{-}n^*$.

The optimization model outlined in Section 3.3 enables computing the optimal trade-off between different options for electrification of urban ferry transport, including vessel size, battery size, sailing speed and recharging options to minimize the sum of the generalized costs of car(/bus) and ferry users as well as the costs of the ferry operator. When the number of ferry users decreases (increases) because of higher (lower) generalized user costs, this increases (decreases) the external costs on the road network which is taken into account in the ferry service optimization. The change in external costs of road transport due to electrification of a ferry service is illustrated by the colored surface in Fig. 1.

Finally, if the electrification of the ferry is imperative but would involve large additional costs, it may be optimal to stop the ferry service altogether. This option is further discussed in Section 5.3.2.

2.2. Placement in the literature

The subsequent section develops an optimization model for optimal planning of a battery-powered urban ferry connection. While the building bricks of the model framework is comparable to other studies on public transport, it combines them with several sub-problems that rarely are considered in public transport planning (Havreetal., 2022). Examples include charging infrastructure planning and mode choice.

In line with many other studies in public transport planning (e.g., Laiand Lo 2004, Arbexand da Cunha 2015, Shangetal.2019), the proposed modeling approach takes both the costs of the operator and passengers into account when planning the vessel service. In line with Soehodoand Koshi(1999), the proposed model also considers crowding costs for passengers. This can be regarded a rare feature of studies on optimal public transport planning (Cederand Sarvi,2007; Shangetal., 2023). We do, however, consider externalities from crowding essential for a model of the urban transport system.

A common feature in comparable studies such as Laiand Lo(2004) and Aslaksenetal. (2020, 2021) is exogenous demand for public transport. Klierand Haase(2015) relax this strong assumption by predicting expected travel times and corresponding demand on the network. Inspired by the study by Klierand Haase(2015), Havreetal.(2022) recently proposed a model for planning of a high-speed ferry service in which the demand for ferry transport depends on the corresponding level of service. This feature is also implemented by the current study. While Havreetal.(2022) use rules of thumb regarding changes in demand, this study advocates using empirically founded *own-price elasticities* combined with generalized costs of travel to evaluate demand for ferry transport subject to the level of service provided.

Another novel feature of the proposed model framework is its consideration of passengers' mode choice (Hartlebetal., 2022). In transport modeling, demand representation is frequently provided by discrete choice models (see e.g. Klierand Haase(2015) and De-Los-Santosetal.(2017) for studies on public transit). They are non-linear and non-convex and have therefore rarely been integrated in optimization problems (Panequeetal., 2021). This study estimates diverted traffic using empirically founded *diversion rates*. They enable capturing key dynamics of mode substitution and induced demand for ferry transport while maintaining a tractable and transparent optimization model.

Studies focusing on decision support problems for zero emission passenger-only ferries are scarce. Planning problems for passenger vessels are among others proposed by Laiand Lo(2004) and Aslaksenetal. (2020, 2021), but none of these studies pay attention to novel operational constraints due to zero emission transport (e.g., limited energy storage capacity and charging/refueling time). Studies on *zero emission* ferry transport are largely limited to Villaetal.(2020) and Havreetal.(2022), but related planning problems for vehicles are more abundant and include among others Rinaldietal.(2018), Roggeetal.(2018), and Zhangetal.(2021). Ritarietal.(2021) study planning of hybrid vessel operations.

Villaetal.(2020) study a charging station location problem for an electric riverboat service. In contrast to this study, the riverboat service caters a rural area with limited grid capacity. Havreetal.(2022) develop a novel MIP model for a planning problem for a battery-powered high-speed ferry service. Their approach combines multiple sub-problems, including infrastructure location, speed selection and vessel scheduling. The MIP model minimizes operator and passenger costs subject to strategic (fleet selection and infrastructure location), tactical (frequency), and operational decisions (sailing pattern). The model proposed in Section3 inherits these properties, but aspects related to passenger flows, infrastructure location, and speed selection are modeled in a more stylized way in the current paper compared to Havreetal.(2022). On the other hand, new elements are added to Havreetal.(2022) novel model framework in this paper to study optimal ferry service design in the urban setting where ferry transport competes with road transportation. First, as previously described, we integrate modal choice between road and ferry transports using empirically founded own-price elasticities and diversion factors to predict changes in demand and mode shifts from/to the passenger vessel service contingent on the frequency of ferry service. Second, minimization of external costs (net of cordon tolls) of diverted road traffic is considered among key priorities of the urban ferry planner as it is a key metric for urban ferry connections relieving road congestion. Third, cost of crowding onboard the ferry is modeled as a function of frequency of service and vessel size provided. Fourth, the level of installed charging power is a decision variable in this analysis. Fifth, extensions of the framework to route selection is considered in a contrafactual scenario analysis in Section5.3.

3. Problem description and mathematical model

This section formalizes the urban ferry transport planning problem and provides a mathematical description of it (formulated as a MIP model). Section3.1 describes the problem together with the assumptions made and the modeling approach. Section3.2 summarizes the notation used for the MIP model, while the MIP model for a battery-powered ferry service is presented in Section3.3. Finally, we describe how this MIP model is adapted to accommodate conventional vessels in Section3.4. This extension enables comparing zero emission and conventional solutions and calculate abatement costs.

3.1. Problem description, assumptions and modeling approach

We consider an urban ferry transport planning problem for a given high-speed ferry connection or route, currently operated by conventional vessels that are considered replaced by zero emission battery-powered vessels. The urban ferry route under consideration is assumed to be a typical commuter route with multiple stops/ports, but with one main port (e.g., in the city center) to/from which most passengers are traveling. To ensure technical feasibility, we assume that the route has a given number of battery chargers along the route, which is either one located in the main port, or at most two. In the second case, one of these battery chargers is in the main port, while the location of the other one is also given.

The key decisions in the urban ferry transport problem include:

i. Number of vessels of which type to use on the given route

ii. Frequency of the given route, i.e., how often it should be operated

iii. Sailing speed along the given route

iv. Installed charging power for the given battery charger(s)

The objective of the urban ferry transport planner is assumed to be minimization of system costs, considering both a) operator costs, b) ferry passenger waiting, travel time, and crowding costs, and c) external costs of road transports caused by traffic diverted to/from the ferry. Key constraints concern ferry passenger capacity, battery and grid capacity, as well as time constraints.

Motivated by our case study (described in Section4), the urban ferry planning problem encompasses three modes of transportation; maritime (ferry) and road transports (car and bus). Planning of the maritime transport subject to implementation of zero emission technology is the primary concern and is consequently subject to detailed modeling, while road transport is modeled solely by means of *diverted traffic* from (to) the ferry to (from) buses and passenger cars.

The basic building brick of the model is passenger flows, defined in terms of passenger flows on O-D pairs connecting the ports along the route. The passengers' preferred route for each O-D pair is defined *a priori* (based on shortest path/feasibility) and is allocated to the set of links $\mathscr{L}$, corresponding to sailing legs along the given route. We assume that the provided ferry capacity must meet the (predefined) demand for ferry transport at each link.

The demand for ferry transport is assumed elastic to generalized prices and consequently affected by changes in the supply of ferry service or fares, all of which can be translated into monetary terms in terms of passengers' *generalized costs of travel*. In our case, passengers' generalized costs stem from waiting, transit time (here also considering crowding) and fares. Using an own-price elasticity,[2] changes in demand (relative to the initial level) subject to changes in generalized costs of ferry transport can be estimated. Utilizing this approach, the demand for ferry transport for different levels of ferry service at each O-D pair is estimated *a priori* and used as an input to the planning problem. By considering changes in the generalized costs of transit from changing the service level (i.e., frequency, vessel size and speed), changes in the demand for ferry transport can be evaluated for each O-D pair. Coupled with the passengers' preferred routes from their origin to their destinations, the demand on each link l subject to the service level defined by vessel type v and the passengers' experienced frequency from operating the service with m vessels that each undertake f roundtrips during the planning period, D_{mfvl}, can consequently be pre-calculated and applied as a parameter in the MIP model. Based on the changes in the demand, external costs of diverted traffic to car (C^{EC}_{mfvij}) and bus (C^{EB}_{mfvij}) transports are computed using *diversion factors* (i.e., changes in the usage of other modes due to changes in demand for a primary mode) alongside marginal external cost estimates.

Use of the two alternative modes is associated with costs due to *congestion*, noise, air pollution, accidents, and road degradation, often referred to as *external costs of transport*. The ferry operator is assumed to internalize the external costs related to diverted traffic to/from the ferry, relative to the initial demand. This approach places an economic value on changes in demand for ferry transport: If additional passengers use the ferry (relative to the initial demand) due to improved supply of ferry services, the operator receives a subsidy (in the form of negative external costs stemming from a reduction in the use of road transport). If fewer passengers use the ferry because of a deterioration of the ferry service, the ferry operator faces a penalty cost for diverted traffic (i.e., due to a ceteris paribus increase in the external costs of road transport).

We assume that the given route's peak period(s) is dimensioning for the strategic decisions mentioned above. Hence, we consider a planning period corresponding to one such peak period (e.g., four hours representing the afternoon peak). The key decisions include fleet acquisition, service frequency and vessel speed. Fleet acquisition is modeled based on a set of predefined candidate vessel types, differing in terms of passenger and energy storage (i.e., battery) capacities. To provide solutions in line with current operational practice, we assume that only one vessel type can be used (although more than one vessel of the chosen type can be selected). Moreover, only candidate vessels with sufficient battery capacity to complete the ferry route subject to the predefined charging locations are considered relevant. Consequently, the number of charging points can affect the set of vessel types that the model can choose from and thereby the strategic fleet decisions. The model can then be solved iteratively for one or two charging points, respectively, and the least costly option is subsequently selected.

Speed and thereby frequency decisions are important for the urban ferry transport problem. For simplification, we assume vessels to operate at a constant (average) speed along the route. This representation of high-speed ferries operating at a constant speed during the transport phase is aligned with previous studies, e.g., Mojarrad et al. (2023). However, we apply an extended set of candidate vessels that accommodates speed choices by defining a number of discrete speeds per candidate vessel type (defined in terms of passenger and battery capacities). The speed and vessel type choices in turn influence energy use. The model also considers a fixed time per call related to starting/stopping the vessel and loading/unloading of passengers.

A key characteristic of battery-powered vessels is that they have limited range and must be charged frequently. The charging time depends on the installed charging power, which is a decision variable in the model. Charging time may in turn influence optimal frequency and waiting times as vessel service operations are prolonged.

To avoid long charging times, a possible strategy for the ferry operator is to top up the battery ahead of a busy service period. The possibility of doing this depends, of course, on the overall schedule of the vessel(s), and thus the time for charging ahead of the peak period. To account for this possibility (but without going into detail regarding preceding vessel activities), we assume that a predefined amount of electricity – defined as a percentage of the battery's overall storage capacity – is available prior to the planning period under consideration.

Another key element of the model is its integration of passenger inconvenience costs due to crowding. Crowding costs are modeled using a piecewise linear function for value of transit time, following the recommendation of Flügel et al. (2020). This ensures that the cost of travel increases with crowding in mass transit. We refer to Section 4 for further details.

3.2. Notation

Before introducing the optimization model, we describe its associated sets, parameters and variables. Note that, due to the significant number of symbols necessary for this model, we use superscripts several places to distinguish parameters and variables from each other. For example, we use C^S and C^J to distinguish labor cost for senior (hence the S superscript) and junior (hence the J superscript) crewmembers.

Sets

$\mathscr{C}$ Set of available charging powers

$\mathscr{V}$ Set of available vessel types

$\mathscr{M}$ Set of candidate fleet sizes, i.e., defining the number of vessels that can be chosen

$\mathscr{F}$ Set of available candidate frequencies (given per vessel)

$\mathscr{N}$ Set of nodes/ports in the considered ferry connection

$\mathscr{L}$ Set of links operated by the considered ferry connection, i.e., the set consists of all links $l = (i, j)$, $i,\ j \in \mathscr{N} |$ i and j represent ports that are visited after each other (i before j) along the route

Parameters

$\overline{T}$ Length of planning period (i.e., the dimensioning peak period)

T_v^R Transit time per roundtrip with a vessel of type v

E_v Energy consumption per roundtrip for a vessel of type v

T^P Fixed time per port call (i.e., for docking and embarking/disembarking passengers)

N Number of charging points along the considered ferry connection/route

C_c^I Cost of installing charging power c (annuitized)

Q_c^I Charging power of infrastructure type c (NOK/MW)

C_v^V Capital costs of a vessel of v (annuitized)

C^E Energy cost per unit (NOK/kWh)

Q_v^P Passenger carrying capacity of a vessel of type v

Q_v^E Energy storage (battery) capacity for a vessel of type v

Q^{INIT} Initial state of charge at the beginning of the planning horizon (in percent)

C^S Labor cost per senior crewmember used on board a vessel

C^J Labor cost per junior crewmember used on board a vessel

L_v^S Minimum safety manning of *senior* crewmembers on a vessel of type v

L_v^J Minimum safety manning of *junior* crewmembers on a vessel of type v

C^T Value of passengers' time (NOK/hour)

D_{mfvl} Demand on link l subject to the service level defined by vessel type v and the frequency given by the frequency per vessel f and the fleet size m

C_{mfvij}^P Waiting and transit time costs for passengers traveling between nodes (ports) i and j, subject to the service level defined by vessel type v and the frequency given by the frequency per vessel f and the fleet size m

C_{mfvij}^{EC} External costs related to diverted traffic to (from) private *car* transport between nodes i and j subject to the service level defined by vessel type v and the frequency given by the frequency per vessel f and the fleet size m

C_{mfvij}^{EB} External costs related to diverted traffic to (from) private *bus* transport between nodes i and j subject to the service level defined by vessel type v and the frequency given by the frequency per vessel f

and the fleet size m

It should be noted that the last four types of parameters are pre-calculated following the procedure with the diversion factors, as described in Section 3.1.

Variables

x_{mfv} Binary variable which takes the value 1 if m vessels of type v operating at a frequency of f (each vessel) is chosen, and 0 otherwise

z_c Binary variable which takes the value 1 if charging power c is chosen, and 0 otherwise

n_v^V Integer variable representing the number of chosen vessels of type v

n_v^F Integer variable representing the effective frequency by vessels of type v, i.e., it defined as the number of vessels of type v multiplied by the chosen frequency f

c^{CT} Charging time costs for passengers in transit

t_c^{TC} Total time spent on charging with charging infrastructure of type c

t^{NC} Net time spent on charging, i.e., the total charging time minus the time for docking and embarking/disembarking passengers

3.3. Mathematical model

In this Section, we define the objective function and the constraints of the urban transport model.

3.3.1. Objective function

The objective of the social ferry planner is to minimize total system costs, represented by objective function (1):

$$\begin{aligned} & N \sum_{c\in\mathscr{C}} C_c^I z_c + \sum_{v\in\mathscr{V}} C_v^V n_v^V + \sum_{v\in\mathscr{V}} C^E E_v n_v^F + \sum_{v\in\mathscr{V}} C^E Q^{INIT} Q_v^E n_v^V \\ & \quad + \sum_{v\in\mathscr{V}} \left(C^S L_v^S + C^J L_v^J\right) n_v^V + \sum_{m\in\mathscr{M}} \sum_{f\in\mathscr{F}} \sum_{v\in\mathscr{V}} \sum_{i\in N} \sum_{j\in N} C_{mfvij}^P x_{mfv} \\ & + c^{CT} \\ & \quad + \sum_{m\in\mathscr{M}} \sum_{f\in\mathscr{F}} \sum_{v\in\mathscr{V}} \sum_{i\in\mathscr{N}} \sum_{j\in\mathscr{N}} \left(C_{mfvij}^{EC} + C_{mfvij}^{EB}\right) x_{mfv} \end{aligned} \tag{1}$$

The first term in objective function (1) comprises the costs of the charging infrastructure, depending on the number of charging points N and the cost of charging power installed, C_c^I. The second term includes the capital costs of the chosen vessel(s), while the next two terms represent the energy costs of sailing and the initial energy level onboard the vessel(s) at the beginning of the planning horizon, respectively. The capital costs (terms 1 and 2) are represented by annuities scaled to the length of the planning horizon. The fifth term in the objective function consists of the crew costs, while the sixth term represents the passengers' waiting and travel costs. The seventh term is the cost of passengers' time associated with vessel charging, i.e., the time beyond the normal time for docking and embarking/disembarking spent on charging, while the last term represents the external costs of diverted traffic, comprising both bus (superscript B) and car (superscript C) travel. The latter costs are, as mentioned in Section 3.1, calculated a priori based on the ferry demand using the diversion factor estimates.

3.3.2. Vessel capacity constraints

$$\sum_{m\in\mathscr{M}}\sum_{f\in\mathscr{F}}\sum_{v\in\mathscr{V}} D_{mfvl}x_{mfv} \leq \sum_{v\in\mathscr{V}} Q_v^P n_v^F, l \in \mathscr{L} \quad (2)$$

Constraints (2) ensure that the capacity provided, given by the right-hand-side (RHS), is sufficient to handle the demand for each link along the ferry route, given by the left-hand-side (LHS). Note again that the demand, given by the parameter D_{mfvl}, is pre-calculated for each of the candidate service levels and vessel types.

3.3.3. Grid capacity constraints

$$\sum_{c\in\mathscr{C}} Q_c^I t_c^{TC} \geq \sum_{v\in\mathscr{V}} E_v n_v^F - \sum_{v\in\mathscr{V}} Q^{INIT} Q_v^E n_v^V, \quad (3)$$

$$t_c^{TC} \leq M^1 z_c, c \in \mathscr{C} \quad (4)$$

Constraint (3) forces the total charging time (LHS) to be long enough to charge the amount of energy needed for sailing the chosen number of roundtrips, adjusted for initial energy storage on board the vessel(s) prior to the planning period under consideration. The charging time also depends on the installed charging power/rate, Q_c^I, given in MW, i.e., choosing a higher charging power from the set of feasible installations (ranging from slow to fast charging) reduces the minimum charging time per energy unit delivered.

Constraints (4) make sure that the charging time for charging power c can only be positive if this level of charging power is chosen. Here, M^1 is a big-M parameter that can be set to the maximum feasible charging time.

3.3.4. Time constraints

$$\sum_{v\in\mathscr{V}} \left(T_v^R + T^P\right) n_v^F + t^{NC} \leq \overline{T} \sum_{v\in\mathscr{V}} n_v^V, \quad (5)$$

$$t^{NC} \geq \sum_{c\in\mathscr{C}} t_c^{TC} - \sum_{v\in\mathscr{V}} T^P n_v^F, \quad (6)$$

Constraint (5) ensures that all vessel operations are performed within the planning horizon. The first term on the LHS gives the total time spent on sailing as well as the time spent in port for docking and embarking/disembarking, while the second term gives the net time for charging. Since the LHS encompasses the time for all vessels (i.e., the overall fleet), the planning horizon must correspondingly be multiplied with the total number of vessels (RHS). Note that all vessels selected (and their assigned operations) are assumed identical, which ensures that the total time of operations is easily obtained by multiplying vessel-specific time by the number of vessels.

Constraint (6) calculates the net time for charging to be the total time for charging minus the time spent for docking and embarking/disembarking (since the latter is also included in the total time spent on charging).

3.3.5. Costs of excessive charging time

$$c^{CT} \geq C^T \sum_{l\in\mathscr{L}^*} D_{mfvl} t^{NC} - M^2 (1 - x_{mfv}), m \in \mathscr{M}, f \in \mathscr{F}, \ v \in \mathscr{V} \tag{7}$$

We assume that passengers *in transit* at the charging point carry the cost of excessive charging time, i.e., the extra time spent on charging beyond the fixed port time for docking and embarking/disembarking. This cost is calculated according to Constraints (7). This cost component is only relevant for the case where two charging points are chosen along the route, as in the case with only one charging point located in the main port, we can assume there are no passengers on board while charging due to the demand mainly going to/from that main port (Aker Brygge in our case study). In the case with two charging points, there will usually be passengers waiting while charging in the second charging port, which will impose a cost according to Constraints (7). The set $\mathscr{L}^*$ which we sum over in these constraints includes only the passengers that actually are on board while charging in the second charging port. We assume there is no crowding during charging, i.e., the base estimate of value of transit time applies.

3.3.6. Fleet, frequency and coupling constraints

$$n_v^F = \sum_{m\in\mathscr{M}} \sum_{f\in\mathscr{F}} m \ f \ x_{mfv}, v \in \mathscr{V} \tag{8}$$

$$n_v^V = \sum_{m\in\mathscr{M}} \sum_{f\in\mathscr{F}} m \ x_{mfv}, v \in \mathscr{V} \tag{9}$$

$$\sum_{m\in\mathscr{M}} \sum_{f\in\mathscr{F}} \sum_{v\in\mathscr{V}} x_{mfv} = 1, \tag{10}$$

$$\sum_{c\in\mathscr{C}} z_c = 1 \tag{11}$$

Constraints (8) calculate the experienced frequency for each vessel type, i.e., the chosen frequency for each vessel multiplied by the number of selected vessels. Constraints (9) calculate the number of vessels of each type. Note that m and f used in these expressions refer to ordinal numbers that count the number of vessels and roundtrips. Constraint (10) ensures that exactly one combination of fleet size, frequency and vessel type is chosen, while Constraint (11) makes sure that exactly one level of charging power is chosen.

3.3.7. Variable definitions

$$z_c \in \{0,1\}, c \in \mathscr{C} \tag{12}$$

$$x_{mfv} \in \{0,1\}, m \in \mathscr{M}, \ f \in \mathscr{F}, \ v \in \mathscr{V} \tag{13}$$

$$n_v^F \geq 0, \ \ \textbf{and integer}, v \in \mathscr{V} \tag{14}$$

$$n_v^V \geq 0, \ \ \textbf{and integer}, v \in \mathscr{V} \tag{15}$$

$$t_c^{TC} \geq 0, c \in \mathscr{C} \tag{16}$$

$$t^{NC} \geq 0, \tag{17}$$

3.4. Model for conventional vessels

We also propose a model for conventional vessels that allows comparing the solutions for battery-powered vessels and conventional ones, and hence calculate carbon abatement costs. The model above is adapted to conventional high-speed vessels by omitting

(a) Charging infrastructure costs ($N \sum_{c \in \mathscr{C}} C_c^I z_c$) and costs of net charging time (c^{TC}) and energy stock ($\sum_{v \in \mathscr{V}} C^E Q^{INIT} Q_v^E n_v^V$) from the objective function (1)

(b) Grid capacity constraints (3)-(4)

(c) Charging time t^{NC} from time constraint (5)

(d) Excess charging time cost constraints (6)-(7)

These terms and constraints regard features that are unique to battery-powered vessels, such as charging power and time. Consequently, a distinction between the costs of operating conventional and battery-powered vessels stems from that the former requires no investment in land-based infrastructure (which is assumed to be sunk costs), while the use of battery-powered vessels requires investment in charging infrastructure. We assume that conventional vessels manage all planned operations within the given planning period without refueling.

4. Case study, data and implementation

The model described in Section3.3 is tested on a case study regarding the planning of the B20 high-speed service connecting the city center of Oslo with its surrounding municipality Asker. The B20 line is a peak-hour service that relieves road traffic on the E18, which is among the busiest road links in Norway. The B20 service calls at the main port Aker Brygge (Oslo city center), as well as Vollen and Slemmestad. A visualization of these ports as well as the E18 highway is provided by Fig.2. It should be emphasized that our model can easily be adapted to other high-speed services with similar characteristics.

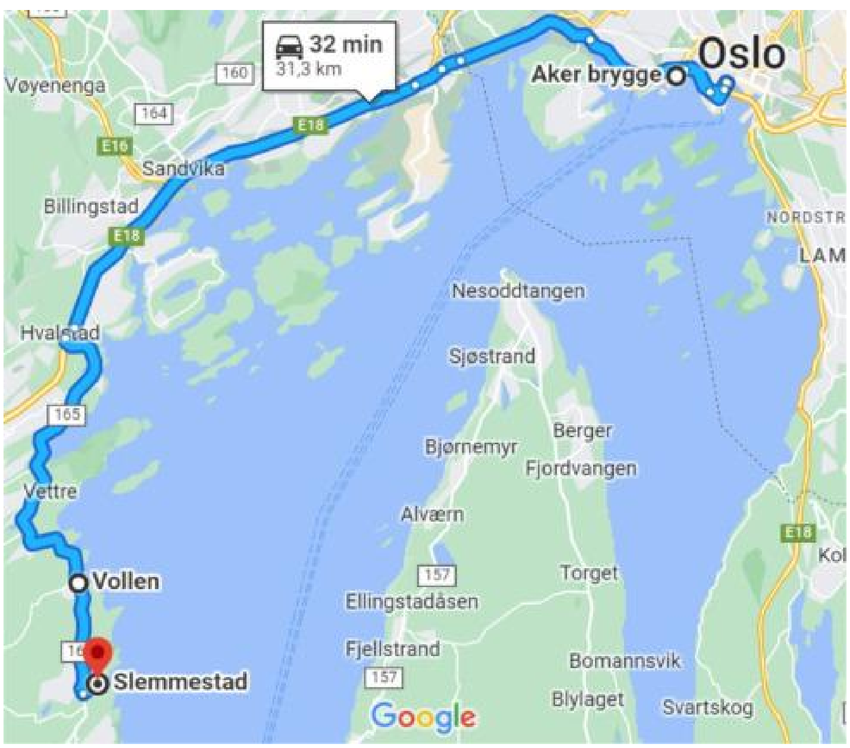

Download : Download high-res image (719KB)
Download : Download full-size image

Fig. 2. The B20 ferry connection. Source: Google maps TM.

The current demand for the ferry service, mapped by Ruter(2020), is a key input to the planning problem. While the B20 line is a typical commuter route that runs both in the morning and in the afternoon, we consider the latter as dimensioning as there are typically more passengers using the ferry service in the afternoon. In this period, most travelers go from Oslo to Vollen or Slemmestad. An O-D matrix mapping the current demand during the afternoon peak period is provided by Table 1.

Table 1. Average number of users of the B20 line in the afternoon peak, per OD-pair.

From/To	**Aker**	**Vollen**	**Slemmestad**
Aker		180	210
Vollen	2		30
Slemmestad	2		

Using Table 1 as point of departure, ferry demand for different levels of service is predicted using an own-price elasticity of −0.3, in line with Jørgensenetal.(2010). This is achieved by computing transit and waiting time costs for different levels of ferry passenger carrying capacity and sailing speed and frequency of service and their corresponding generalized costs of travel. For each instance, the change in demand relative to the current demand is estimated by multiplying the own-price elasticity estimate with the change in generalized costs of travel, relative to current generalized costs of travel. Based on changes in the demand for ferry services (relative to the base scenario) with changes in the frequency of service, diversion factors of 0.471 and 0.500 are used to calculate diverted traffic to/from car and bus travel, respectively. These estimates are based on Flügeletal.(2018).

Diverted traffic is subsequently translated into changes in external costs of road transport due to changes in the ferry service design. External costs of traffic diverted from (to) the ferry to (from) road transport are based on the latest estimates of external costs of rush-hour driving (Rødsethetal., 2019), weighted by energy carrier using the current fleet shares in the Oslo-region as weights. Damage costs (i.e., costs related to traffic congestion, noise, air pollution, accidents, and road degradation) of car and bus transport equal 4.83 and 0.86 NOK per kilometer (per passenger), respectively, where the latter assumes a utilization rate of 15 passengers per bus. External costs of car transport are calculated by subtracting cordon tolls from the estimated damage costs. Tolls amount to 30 NOK for traffic leaving the city center and 60 NOK for traffic entering the city center, again assuming a weighted average of tariffs for different vehicle types.

Ferry transit time costs are computed based on predicted demand for each service level. They follow Flügeletal.(2020), using a (base) value of time of 128 (2021-)NOK/hour per passenger. A piecewise linear function for value of transit time in terms of capacity utilization (i.e., number of passengers relative to the passenger capacity of a ferry) is applied to appraise crowding. An example of transit time costs per passenger in function of capacity utilization, in the case where the vessel under consideration is certified to carry up to 50 passengers, is provided by Fig. 3. Tipping points for the transit time costs are at 40 and 80 percent of the total capacity, respectively.

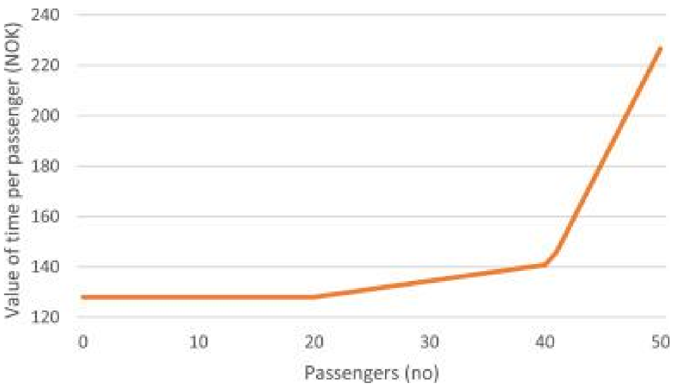

Fig. 3. Value of transit time (NOK/hour) per passenger for a vessel certified for up to 50 pax.

For battery-powered ferries, charging time exceeding the standard docking time is also assumed to cause disutility for passengers *in transit*. This applies only in the case where charging infrastructure is installed at Slemmestad in addition to at the service's main port at Aker Brygge, as charging at Slemmestad affects passengers traveling from Vollen to Aker Brygge. Their disutility is appraised at the base estimate of value of time assuming no crowding during charging. The base time for loading/unloading passengers is set equal to three minutes per quay, in line with Havreetal.(2022).

In addition to transit time costs, generalized costs are assumed to comprise waiting time costs and (exogenous given) fares. Average waiting time per passenger is assumed half of the ratio between the duration of the planning horizon and frequency (i.e., the number of times a port is visited during the planning horizon). The value of waiting time is assumed 1.5 times the base estimate of value of time following Wardmanetal.(2016). Fares are set equal to current zonal prices in the Oslo region and amount to 64 NOK between Aker Brygge and Vollen and Vollen and Slemmestad and 89 NOK between Aker Brygge and Slemmestad.

The operating costs of the ferry are assumed to comprise energy and labor costs, while capital costs relate to vessels and charging infrastructure. The cost profile of operations depends on the type and number of vessels in use. The set of candidate vessels to choose from is presented by TableA1 in Appendix A, which is based on Havreetal.(2022) for battery-powered (ZE) vessels and on Tveteretal.(2020) for the conventional (MGO) vessel. Minimum safety manning is estimated using Data Envelopment Analysis (Charnesetal., 1978) on a dataset of existing high-speed vessels under the assumption that manning certification does not change with ZE technology. Labor is classified into senior (i.e., officers) and junior crewmembers.

The candidate vessel types differ in terms of passenger capacity, battery capacity, and sailing speed, and therefore with regards to minimum safety manning and energy consumption. Following Tveteretal.(2020) we assume day rates of 4 136 and 3 115 NOK per person for senior and junior crewmembers, respectively. Energy costs are set to 5 300 NOK per metric ton for conventional vessels and 0.5688 NOK per kWh for electricity. These estimates are in accordance with the Norwegian Government's investigation into measures for meeting emission targets set by the Paris agreement (NorwegianEnvironment Agency,2020). Capital costs for vessels and chargers are modeled as day chartering rates based on annuities. Note that capital costs are assumed different for conventional and battery-powered vessels: Based on advice from the maritime consultant involved in our research project, we assume that the only difference between capital expenditures of conventional and battery-powered vessels is that the former does not carry the cost of batteries, which in Havreetal.(2022) is assumed to amount to 6 900 NOK/kWh of energy storage. For each vessel type, we apply seven discrete speeds, i.e., 15 knots (slow speed) and integers from 20 to 25 knots, where 25 knots is that maximal allowed speed in the Oslo fjord.

Following Tveteretal.(2020) and Rødsethetal.(2022), vessels and chargers are assumed to have an economic lifespan of 15 and 20 years, respectively, and the interest rate is set to 4 percent which is standard in cost benefit analysis in the transport sector in Norway.

The B20 route is currently operated by one vessel that undertakes three roundtrips during the 4h planning period under consideration. The current vessel type is labeled **v1** in TableA1, where we see strong economies of scale with respect to vessel size and diseconomies of scale with respect to speed. For the initial computations (subsequently referred to as the "base scenario"), we assume that up to two vessels, each operating up to three roundtrips during the planning period, constitutes a relevant size of the choice set. The set of feasible charging powers are assumed to range from 1 to 5 MW (enabling the choice between slow and fast charging), while initial state of charge of the battery is assumed to be 40 percent.

An overview of key parameters in the model is provided by Tables2 and A1. The latter covers parameters that are specific to a vessel type.

Table 2. Summary of key parameters.

Parameter	**Value**	**Parameter**	**Value**
$\overline{T}$	4 h	Own-price elasticity	- 0.300
T^P	3 min	Diversion factor car	0.471
C^E	5 300 NOK/t diesel; 0.570 NOK/kWh electricity	Diversion factor bus	0.500
Q^{INIT}	0.400	Damage cost car	4.830 NOK/km
C^S	4 136 NOK/day	Damage cost bus	0.860 NOK/km
C^J	3 115 NOK/day	Cordon tolls	30 (leaving); 60 (entering)
C^T	128 NOK/hr	Fares	64; 89 (Aker-Slemmestad)
Waiting time	1.5 (scalar)		

We solve three optimization problems iteratively: Two problems for ZE vessels with one and two charging locations, respectively, and one problem for conventional vessel. Each problem is solved to optimality within a few seconds. For the base scenario, the battery-powered vessel models contain 675 and 1 025 equations and 607 and 922 variables, respectively, while the model for conventional vessels contains 151 equations and 325 variables. The model is solved in GAMS using the Xpress Solver on a Dell laptop with IntelCore i7–10,510U CPU @ 1.80GHz 2.30GHz processor with 16 GB RAM. The average solution time for the base scenario is 0.03s per individual model.

5. Computational results

This section presents the numerical results. It starts with the base scenario (i.e., optimization of the current route), followed by sensitivity testing and contrafactual scenarios.

5.1. Base scenario

Table 3 presents characteristics of the optimal solutions for the base scenario for conventional and battery-powered high-speed ferries, respectively. Herein, we contrast these results to the current service, which was outlined in Section 4. A further investigation and comparison to the current service can also be found in Section 5.2.1.

Table 3. Characteristics of the base scenario.

	Conventional	**Battery-powered**
Vessels (no)	1	1
− Passenger capacity (no)	200	200
− Battery capacity (kWh)	–	3 000
− Speed (knot)	25	25
Frequency (no)	3	3
Passengers (no)	642	642
Charging points (no)	–	1
− Installed capacity (MW)	–	3
CO_2 emissions (t)	2.7	–

For the (optimized) base scenarios, both for conventional and for battery-powered high-speed ferries, one vessel operating three roundtrips in the planning period is selected, which corresponds to the current frequency. Hence, maintaining the current timetable is suitable for an optimized service. However, since the optimized services operate at an average speed of 25 knots as opposed to 21 knots for the current service – which reduces ferry passengers' transit time costs – there is a slight increase in the number of ferry users relative to the current demand, which in turn contributes to a small reduction in the external costs of road transport.

The finding regarding speed choice is counter to the results of Havre et al. (2022), who showed that energy saving and thereby speed reductions are paramount for ZE vessel operations. However, contrary to this study, reduction of costs due to crowding and excessive charging time were not among the objectives of Havre et al.'s study that focuses on rural as opposed to urban transport.

Note that to accommodate the high speed, a vessel with a medium battery size (i.e., 3 000 kWh) is selected, which adds to the capital costs of the *zero emission* vessel service. However, because of the battery range, installing only one battery charger at Aker Brygge suffices for managing planned operations. This implies that no passengers experience prolonged travel time due to charging. This would, on the contrary, be the case if an additional charging infrastructure had been installed at Slemmestad, where charging would prolong the travel time of passengers in transit from Vollen to Aker Brygge.

The optimal installed charging power is 3 MW. This is slightly higher than the installed capacity of the world's first battery-powered high-speed vessel Medstraum, but well within the range of installed capacities at existing ferry connections in Norway; cf Section.0.

Fig.4 visualizes the cost structure of the base scenario for diesel and battery-powered vessels, respectively. All costs are in (rounded) kNOK for the planning period. The figure clearly shows that the main cost component relates to passengers. It is also noteworthy that the operator costs of the battery-powered vessel (40 kNOK) are higher than the operator costs of the conventional vessels (32 kNOK) – especially because the capital costs are increased with the transition to ZE. This is related to the need for investing in both energy storage and charging infrastructure.

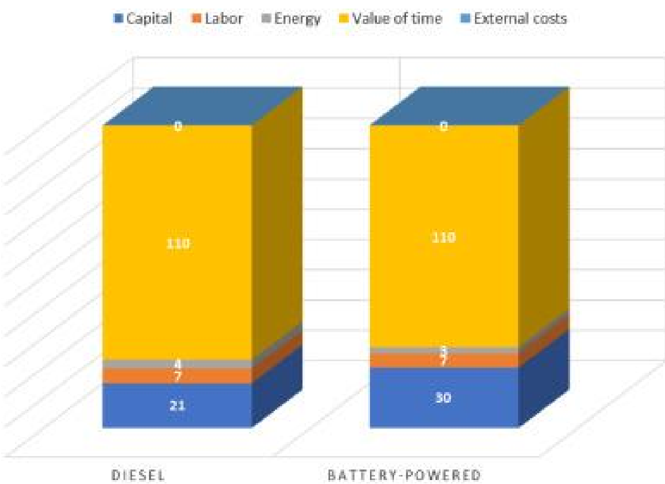

Download : Download high-res image (140KB)
Download : Download full-size image

Fig. 4. Cost structure of base scenario.

The gap between system costs for diesel and battery-powered vessels amounts to 6 984 NOK for the 4h planning horizon. While the transition to zero emission vessel increases the cost of the ferry operations (evaluated at current fuel prices, that reflect the current carbon pricing of maritime transport), it carries the benefit of saving 2.7 tons of CO_2 within the planning period (cf., Table3). This emission reduction is estimated assuming a conversion rate of 3.2kg CO_2 per kg diesel. Consequently, the total abatement costs per planning period (amounting to 6 984 NOK) can be translated into an abatement cost of 2 563 NOK per ton of CO_2 by dividing the total abatement costs by the tons of CO_2 saved.

Thus, cost of electrification of the B20 line is found to be higher than the Norwegian government's estimate of the social cost of carbon at 2 000 NOK per ton in 2030. The zero emission initiative is, however, closer to passing the cost-benefit test compared to the results obtained by Havreetal.(2022) for rural connections where abatement costs ranged between 3 000 and 18 000 NOK per ton. However, our results show that fuel costs must increase from 5 300 NOK per ton of diesel to 13 590 NOK per ton of diesel for the costs of diesel vessel operations to become *at par* with the costs of battery-powered vessel operations. This corresponds to an increase in the fuel costs of about 3 000 NOK per ton of CO_2 abated. In this case, the energy costs of diesel ferry operations increase from 4 kNOK (cf., Fig.4) to 11 kNOK.

Note that external costs (of road transport) are 0 in Fig.4 because numbers are rounded. Detailed accounts show that external costs are −274 NOK due to passenger being diverted from road transport to the ferry when a swifter transport service is provided (i.e., because the optimized average speed is 25 knots, while the existing service operates at an average of 21 knots, as previously described).

5.2. Sensitivity tests

The base scenario results indicate that parameters related to energy consumption are important for the system costs of ZE vessel operations. This section consequently undertakes sensitivity testing of key parameters related to the energy input. A summary of the tests and their results are provided by Table4.

Table 4. Summary of sensitivity tests.

Test	Criterion	Total cost (kNOK)	Abatement cost (kNOK)
Initial vessel	Vessel type v1	150	0
State of charge	0%	151	8
State of charge	80%	150	6
Maximal installed capacity	2 MW	162	19
Energy price	7000/3.1NOK	160	15

5.2.1. Initial vessel

The first test evaluates the scope for cost reduction by optimizing the existing service. It compares the (optimized) costs of zero emission vessel operation to the cost of an (sub)optimized conventional ferry service operated with the current vessel type (**v1**). This vessel has a carrying capacity of 250 passengers and travels at an average speed of 21 knots. We refer to TableA1 for details regarding this vessel.

The system costs of diesel ferry operations amount to 150 kNOK when vessel type **v1** is used. For comparison, system costs of the optimized diesel and battery-powered operations presented in Fig.4 are 143 and 150 kNOK, respectively. Consequently, we estimate an economic loss of about 7 kNOK when comparing the system cost of the diesel service using vessel type **v1** to the optimized diesel ferry service. Comparing the diesel service using vessel type **v1** to the optimized battery-powered service, we find a cost saving for the battery-powered service amounting to –440 NOK (rounded to 0 kNOK in Table4) in total for the 4h planning period, thereby illustrating the prominent role of strategic decisions in reducing the costs of vessel operations.

This result provides some hope for the case for zero emission transport on the Aker brygge-Vollen-Slemmestad connection. As the existing vessel operating the connection is sub-optimal for the current service, there is scope for reducing costs by optimizing a battery-powered ferry transport service. Hence, strategies to mitigate inefficiencies in vessel operations should also be considered when mapping abatement costs.

Examining the cost breakdown for this case, we find that the key difference between system costs of the sub-optimal and optimized diesel ferry services stems from differences in capital costs. Second, there are cost saving in terms of energy use from choosing a smaller and lighter vessel. Third, as the sub-optimal service operates at a lower speed compared to the optimized service, cost attributed to passengers' travel and waiting times are higher and reduction in external costs of road transport from traffic diversion is smaller than for the optimized service.

5.2.2. State of charge

For the second test, we assume that the state of charge prior to the planning horizon is either 0 (i.e., the total amount of energy needed during the planning horizon must be charged during the planning period) or 80 percent. In these cases, abatement costs – here comparing optimal solutions for conventional and battery-powered vessels – are *8* and *6 kNOK*, respectively, while the abatement costs are 7 kNOK in the base scenario. Hence, the results are fairly invariant to the modeling of initial energy stock.

5.2.3. Maximal installed capacity

For the third test, we assume that the maximal installed capacity is *2* MW (as opposed to 5 MW). In this case, abatement costs – comparing optimal solutions for conventional and battery-powered vessels – are *19 kNOK*. This suggests that access to fast charging is important for reducing the costs of battery-powered vessel operations. *Grid capacity* can thus be considered a key barrier for diffusion of zero emission technologies.

5.2.4. Energy price

For the final test, we assume an electricity price of 3.1 NOK per kWh and an MGO price of 7 000 per metric ton as in Havre et al. (2022). This compares with energy costs of 0.5688 NOK per kWh and 5 300 NOK per metric ton for electricity and MGO, respectively, used for the base scenario. In this case, abatement cost – comparing optimal solutions for conventional and battery-powered vessels – is 15 *kNOK*, and the costs from transition to zero emission is more than doubled compared to the base scenario. The economics of zero emission vessels are sensitive to developments of energy prices: high renewable energy prices make the case for electric ferries much more difficult.

5.3. Counterfactual scenarios

Thus far, we have considered the costs of zero emission operations of the existing B20 service. In this section, we study economic implications of implementing fundamental changes to the existing route, encompassing

(a) Route changes

(b) Closing of the B20 service

5.3.1. Route scenario

An alternative operational measure to reduce system costs of the ferry service can be to alter its route and to offer replacement bus services to ports that are omitted from the ferry route. To study its economic implications, we model *hypothetical* ferry routes between a) Aker Brygge and Vollen and b) Aker Brygge and Slemmestad. We will subsequently refer to these as the a) Vollen and b) Slemmestad scenarios. In both cases, we assume a replacement bus service between Slemmestad and Vollen. These scenarios enable reducing the energy consumption of the ferry by reducing the roundtrip length, but at the expense of transit costs for passengers from Slemmestad or Vollen. The alternative service to Vollen (Slemmestad) benefits passengers traveling from Vollen (Slemmestad), who will experience a direct service to Aker Brygge.

Table 5 compares the cost minimums for the base and alternative route scenarios. It shows that the system costs can on average be reduced by 5.2 and 6.7 percent for conventional and battery-powered vessels, respectively, by implementing the shorter vessel routes. A key driver behind the reduced costs is that shortening sea distance affects strategic decisions: In both alternative scenarios, the model selects a battery-powered vessel with a lower passenger capacity (150 pax) and battery size (2 000 kWh) than in the base scenario. For the Vollen scenario, the model also selects a lower charging power (2 MW) than in the base scenario.

Table 5. Comparison of cost minimums for base and route scenarios.

	Costs (kNOK) Base scenario	Costs (kNOK) Vollen scenario	Costs (kNOK) Slemmestad scenario	Avg. cost reduction (kNOK)
Conventional	143	134	137	−7.5
Battery-powered	150	138	142	−10
Abatement costs	7	4	5	

Route changes can be pertinent for planning of battery-powered vessel services, serving as an instrument to circumvent constraints related to energy storage and limited range. If we compare the cost of zero emission operations under the alternative route (138 kNOK for the Vollen scenario and 142 kNOK for the Slemmestad scenario) to the costs of operating the current route with conventional vessels (143 kNOK) we find negative abatement costs when enabling route changes. Route planning should consequently be considered an instrument in promoting cost-effective transition to green maritime transport.

5.3.2. Closing scenario

In this scenario, we consider the external costs that arise from diverted traffic when the B20 line shuts down. Using the diversion factors defined in Section 4, we find that total external costs of diverted traffic sums to 32.8 kNOK for the planning period. This is substantially less than the system costs of the ferry service, thus suggesting that the B20 line is not economically viable on the grounds of correcting externalities of road transport.

6. Summary and conclusions

This paper has studied technical and economic feasibilities of a zero emission high-speed ferry connection in Norway's capital Oslo. The ferry connection under consideration is in close competition with road and bus transport, alleviating traffic externalities on the crowded E18 highway into the heart of Oslo. This aspect is integrated into the optimization-based planning tool for ferry transport operations developed in this paper. Whilst building on the novel model by Havreetal.(2022), this paper extends their contributions by considering diversion of ferry traffic, external costs of road traffic and potentials to reduce ferry system costs by modifying current routes.

In line with Havreetal.(2022), the current paper finds that electrification of the current route does not pass the cost-benefit test. Further investigation shows that this conclusion is circumvented when acknowledging inefficiencies in current operations, which is often neglected by planning studies. Moving from an inefficient towards an optimized service can lead to substantial environmental and economic gains, which should be carefully considered by planners. Mitigation of inefficiencies should also be acknowledged by environmental policies, e.g., when setting targets for transition to low- and zero emission transport.

The current paper identifies grid capacity as a substantial barrier for diffusion of battery-powered vessels. This can be particularly challenging in remote locations but is also likely to apply in the urban setting where several appliances compete for power. Technical solutions that reduce the need for instantaneous energy transfer, e.g., through use of a battery bank, is therefore needed to enable cost-effective transport electrification. The economic case for battery-powered vessels is also highly dependent on the development of (relative) energy prices. The transition to zero emission transport inevitably brings the energy and transport sectors closer together which makes holistic transport and energy policies pertinent (Wangsnessetal., 2021).

This paper further investigates cost savings from route planning, considering a shorter ferry route with replacement transport as an alternative to the existing route. This investigation shows that route planning can be effective to mitigate or circumvent abatement costs associated with the transition to zero emission transport. We consequently advise decisions makers in the public transport sector in Norway to revise their strategies of upholding existing routes and services under zero emission transport, and rather to embrace changes in cost structures and optimal public transport supply that follow from the sought energy transition.

The optimization model developed in this paper encompasses key characteristics of an urban transport market, including in-vessel crowding, road congestion and mode competition. It can consequently be generalized to analyze optimal ferry design in other urban case studies. While the case study analyzed in this paper contains a small network and therefore can be solved to optimality within a few seconds using commercial solvers, other applications with an extensive network may require the development of efficient algorithms for solving the problem. A heuristic Decomposition Based method for optimal planning of high-speed ferry connections is presented in Havreetal.(2023).

In this study, separate models for battery-powered and conventional vessels are developed to compare the immediate cost and benefits of adoption of zero emission vessel technology, which is an essential input to Norwegian policies that request a full-fledged energy transition by 2025. For other cases with a gradual phase-in of zero emission technology, an extension of the current model that considers an optimal fleet mix among battery-powered and conventional ferries and optimal timing of investments is advised. We leave this for further research.

Declaration of Competing Interest

The authors declare the following financial interests/personal relationships which may be considered as potential competing interests:

Kenneth Løvold Rødseth reports financial support was provided by Research Council of Norway.

Kjetil Fagerholt is serving in an editorial capacity for Maritime Transport Research.

Acknowledgement

This paper is an outlet from the research projects *enabling Zero Emission passenger Vessel Services* (ZEVS) and *PLATform for Open and Nationally accessible climate policy knowledge* (PLATON), both funded by the Research Council of Norway (Grant no. 320659 and 295789). The authors are indebted to the ZEVS project's many user partners for their input to parameters, case studies and modeling. Support from Institute for Energy Technology and ship builder Brødrene Aa has been vital to our research. We are also grateful to the reviewers, whose comments and suggestions have helped us to improve the paper.

Appendix A

(Table A1)

Table A1. List of candidate vessels.

	Energy carrier	Passenger Capacity (Pax)	Battery Capacity (kWh)	Average Speed (Knots)	Capital costs (mNOK)	Crew Senior (no)	Crew Junior (no)	Energy consumption (l/kWh)
v1	MGO	250		21	105	3	1	0.0072
v2	MGO	100		15	87	1	2	0.0039
v3	MGO	100		20	87	1	2	0.0044
v4	MGO	100		21	87	1	2	0.0045
v5	MGO	100		22	87	1	2	0.0046
v6	MGO	100		23	87	1	2	0.0047
v7	MGO	100		24	87	1	2	0.0048
v8	MGO	100		25	87	1	2	0.0049
v9	MGO	150		15	88	2	1	0.0048
v10	MGO	150		20	88	2	1	0.0054
v11	MGO	150		21	88	2	1	0.0055

	Energy carrier	Passenger Capacity (Pax)	Battery Capacity (kWh)	Average Speed (Knots)	Capital costs (mNOK)	Crew Senior (no)	Crew Junior (no)	Energy consumption (l/kWh)
v12	MGO	150		22	88	2	1	0.0057
v13	MGO	150		23	88	2	1	0.0058
v14	MGO	150		24	88	2	1	0.0059
v15	MGO	150		25	88	2	1	0.0060
v16	MGO	200		15	89	2	2	0.0056
v17	MGO	200		20	89	2	2	0.0063
v18	MGO	200		21	89	2	2	0.0064
v19	MGO	200		22	89	2	2	0.0066
v20	MGO	200		23	89	2	2	0.0067
v21	MGO	200		24	89	2	2	0.0068
v22	MGO	200		25	89	2	2	0.0069
v23	MGO	250		15	105	3	1	0.0062
v24	MGO	250		20	105	3	1	0.0071
v25	MGO	250		21	105	3	1	0.0072
v26	MGO	250		22	105	3	1	0.0074
v27	MGO	250		23	105	3	1	0.0075
v28	MGO	250		24	105	3	1	0.0077
v29	MGO	250		25	105	3	1	0.0078
v30	MGO	300		15	106	3	1	0.0068
v31	MGO	300		20	106	3	1	0.0078
v32	MGO	300		21	106	3	1	0.0079
v33	MGO	300		22	106	3	1	0.0081
v34	MGO	300		23	106	3	1	0.0083
v35	MGO	300		24	106	3	1	0.0084
v36	MGO	300		25	106	3	1	0.0086
v37	ZE	100	1000	15	94	1	2	472
v38	ZE	100	1000	20	94	1	2	805
v39	ZE	100	1000	21	94	1	2	885
v40	ZE	100	1000	22	94	1	2	965

	Energy carrier	Passenger Capacity (Pax)	Battery Capacity (kWh)	Average Speed (Knots)	Capital costs (mNOK)	Crew Senior (no)	Crew Junior (no)	Energy consumption (l/kWh)
v41	ZE	100	1000	23	94	1	2	1045
v42	ZE	100	1000	24	94	1	2	1125
v43	ZE	100	1000	25	94	1	2	1205
v44	ZE	100	2000	15	101	1	2	517
v45	ZE	100	2000	20	101	1	2	873
v46	ZE	100	2000	21	101	1	2	956
v47	ZE	100	2000	22	101	1	2	1039
v48	ZE	100	2000	23	101	1	2	1121
v49	ZE	100	2000	24	101	1	2	1204
v50	ZE	100	2000	25	101	1	2	1287
v51	ZE	100	3000	15	108	1	2	564
v52	ZE	100	3000	20	108	1	2	946
v53	ZE	100	3000	21	108	1	2	1031
v54	ZE	100	3000	22	108	1	2	1115
v55	ZE	100	3000	23	108	1	2	1200
v56	ZE	100	3000	24	108	1	2	1284
v57	ZE	100	3000	25	108	1	2	1369
v58	ZE	150	1000	15	95	2	1	544
v59	ZE	150	1000	20	95	2	1	915
v60	ZE	150	1000	21	95	2	1	999
v61	ZE	150	1000	22	95	2	1	1083
v62	ZE	150	1000	23	95	2	1	1167
v63	ZE	150	1000	24	95	2	1	1251
v64	ZE	150	1000	25	95	2	1	1335
v65	ZE	150	2000	15	102	2	1	593
v66	ZE	150	2000	20	102	2	1	990
v67	ZE	150	2000	21	102	2	1	1076
v68	ZE	150	2000	22	102	2	1	1161
v69	ZE	150	2000	23	102	2	1	1247

	Energy carrier	Passenger Capacity (Pax)	Battery Capacity (kWh)	Average Speed (Knots)	Capital costs (mNOK)	Crew Senior (no)	Crew Junior (no)	Energy consumption (l/kWh)
v70	ZE	150	2000	24	102	2	1	1332
v71	ZE	150	2000	25	102	2	1	1418
v72	ZE	150	3000	15	109	2	1	644
v73	ZE	150	3000	20	109	2	1	1068
v74	ZE	150	3000	21	109	2	1	1155
v75	ZE	150	3000	22	109	2	1	1242
v76	ZE	150	3000	23	109	2	1	1329
v77	ZE	150	3000	24	109	2	1	1416
v78	ZE	150	3000	25	109	2	1	1503
v79	ZE	200	1000	15	96	2	2	622
v80	ZE	200	1000	20	96	2	2	1035
v81	ZE	200	1000	21	96	2	2	1121
v82	ZE	200	1000	22	96	2	2	1208
v83	ZE	200	1000	23	96	2	2	1294
v84	ZE	200	1000	24	96	2	2	1381
v85	ZE	200	1000	25	96	2	2	1467
v86	ZE	200	2000	15	103	2	2	674
v87	ZE	200	2000	20	103	2	2	1115
v88	ZE	200	2000	21	103	2	2	1203
v89	ZE	200	2000	22	103	2	2	1290
v90	ZE	200	2000	23	103	2	2	1378
v91	ZE	200	2000	24	103	2	2	1465
v92	ZE	200	2000	25	103	2	2	1553
v93	ZE	200	3000	15	110	2	2	729
v94	ZE	200	3000	20	110	2	2	1199
v95	ZE	200	3000	21	110	2	2	1287
v96	ZE	200	3000	22	110	2	2	1375
v97	ZE	200	3000	23	110	2	2	1464
v98	ZE	200	3000	24	110	2	2	1552

	Energy carrier	Passenger Capacity (Pax)	Battery Capacity (kWh)	Average Speed (Knots)	Capital costs (mNOK)	Crew Senior (no)	Crew Junior (no)	Energy consumption (l/kWh)
v99	ZE	200	3000	25	110	2	2	1640
v100	ZE	250	2000	15	119	3	1	376
v101	ZE	250	2000	20	119	3	1	1023
v102	ZE	250	2000	21	119	3	1	1122
v103	ZE	250	2000	22	119	3	1	1221
v104	ZE	250	2000	23	119	3	1	1320
v105	ZE	250	2000	24	119	3	1	1419
v106	ZE	250	2000	25	119	3	1	1518
v107	ZE	250	3500	15	130	3	1	406
v108	ZE	250	3500	20	130	3	1	1091
v109	ZE	250	3500	21	130	3	1	1196
v110	ZE	250	3500	22	130	3	1	1302
v111	ZE	250	3500	23	130	3	1	1407
v112	ZE	250	3500	24	130	3	1	1513
v113	ZE	250	3500	25	130	3	1	1618
v114	ZE	250	5000	15	140	3	1	438
v115	ZE	250	5000	20	140	3	1	1163
v116	ZE	250	5000	21	140	3	1	1275
v117	ZE	250	5000	22	140	3	1	1386
v118	ZE	250	5000	23	140	3	1	1498
v119	ZE	250	5000	24	140	3	1	1609
v120	ZE	250	5000	25	140	3	1	1721
v121	ZE	300	2000	15	120	3	1	408
v122	ZE	300	2000	20	120	3	1	1095
v123	ZE	300	2000	21	120	3	1	1201
v124	ZE	300	2000	22	120	3	1	1307
v125	ZE	300	2000	23	120	3	1	1412
v126	ZE	300	2000	24	120	3	1	1518
v127	ZE	300	2000	25	120	3	1	1624

	Energy carrier	Passenger Capacity (Pax)	Battery Capacity (kWh)	Average Speed (Knots)	Capital costs (mNOK)	Crew Senior (no)	Crew Junior (no)	Energy consumption (l/kWh)
v128	ZE	300	3500	15	130	3	1	440
v129	ZE	300	3500	20	130	3	1	1167
v130	ZE	300	3500	21	130	3	1	1279
v131	ZE	300	3500	22	130	3	1	1391
v132	ZE	300	3500	23	130	3	1	1503
v133	ZE	300	3500	24	130	3	1	1615
v134	ZE	300	3500	25	130	3	1	1727
v135	ZE	300	5000	15	141	3	1	474
v136	ZE	300	5000	20	141	3	1	1241
v137	ZE	300	5000	21	141	3	1	1359
v138	ZE	300	5000	22	141	3	1	1478
v139	ZE	300	5000	23	141	3	1	1596
v140	ZE	300	5000	24	141	3	1	1715
v141	ZE	300	5000	25	141	3	1	1833

References

Arbex and da Cunha, 2015 R.O. Arbex, C.B. da Cunha
Efficient transit network design and frequencies setting multi-objective optimization by alternating objective genetic algorithm
Transp. Res. Part B Methodol., 81 (2015), pp. 355-376
View PDF   View article   View in Scopus ↗   Google Scholar ↗

Aslaksen et al., 2021 I.E. Aslaksen, E. Svanberg, K. Fagerholt, L.C. Johnsen, F. Meisel
A combined dial-a-ride and fixed schedule ferry service for coastal cities
Transp. Res. Part A Policy Pract., 153 (2021), pp. 306-325
View PDF   View article   View in Scopus ↗   Google Scholar ↗

Aslaksen et al., 2020 I.E. Aslaksen, E. Svanberg, K. Fagerholt, L.C. Johnsen, F. Meisel
Ferry service network design for the Kiel fjord
Proceedings of the Lecture Notes in Computer Science LNCS, 12433 (2020), pp. 36-51
CrossRef ↗   View in Scopus ↗   Google Scholar ↗

Ceder and Sarvi, 2007 A. Ceder, M. Sarvi
Design and evaluation of passenger ferry routes
J. Public Transp., 10 (2007), pp. 59-79
View PDF View article CrossRef Google Scholar

Charnes et al., 1978 A. Charnes, W.W. Cooper, E. Rhodes
Measuring the efficiency of decision making units
Eur. J. Oper. Res., 2 (1978), pp. 429-444
View PDF View article View in Scopus Google Scholar

De-Los-Santos et al., 2017 A. De-Los-Santos, G. Laporte, J.A. Mesa, F. Perea
The railway line frequency and size setting problem
Public Transp., 9 (2017), pp. 33-53
CrossRef View in Scopus Google Scholar

De Palma et al., 2015 A. De Palma, M. Kilaini, S. Proost
Discomfort in mass transit and its implication for scheduling and pricing
Transp. Res. Part B Methodol., 71 (2015), pp. 1-18
View PDF View article CrossRef View in Scopus Google Scholar

Eide et al., 2018 M.S. Eide, Ø. Endresen, R. Hagman, A. Mjelde, S. Pedersen, J. Aarhaug
Fylkeskommunenes Klimagassutslipp fra Lokale Ruter (in Norwegian)
Menon-Publikasjon (2018)
nr. 22/2018
Google Scholar

Flügel et al., 2018 S. Flügel, N. Fearnley, J. Toner
What factors affect cross-modal substitution?–Evidences from the Oslo Area
Int. J. Transp. Dev. Integr., 2 (2018), pp. 11-29
View in Scopus Google Scholar

Flügel et al., 2020 S. Flügel, A.H. Halse, N. Hulleberg, G.N. Jordbakke, K. Veisten, H.B. Sundfør, M. Kouwenhoven
Verdsetting av Reisetid og Tidsavhengige Faktorer (in Norwegian)
Transportøkonomisk Institutt, Oslo (2020)
TØI Report 1762/2020
Google Scholar

Frost and Brooks, 2021 J.D. Frost, M.R. Brooks
Seeking economic and social success with sustainable urban ferry services
IN:
The Routledge Handbook of Public Transport, Routledge, London (2021)
Google Scholar

Hartleb et al., 2022 J. Hartleb, M. Schmidt, D. Huisman, M. Friedrich

Modeling and solving line planning with mode choice

Transp. Sci., 57 (2022), pp. 336-350

Google Scholar ↗

Havre et al., 2022 H.F. Havre, U. Lien, M.M. Ness, K. Fagerholt, K.L. Rødseth

Cost-effective planning and abatement costs of battery-powered passenger vessel services

Transp. Res. Part D Transp. Environ., 113 (2022), Article 103495

View PDF View article View in Scopus ↗ Google Scholar ↗

Havre et al., 2023 Havre, H.F., Lien, U. Ness, M.M., Fagerholt, K. & K.L. Rødseth (2023) Optimal route to battery electric high-speed vessel services. Available at SSRN: https://ssrn.com/abstract=4330381 ↗ or doi:10.2139/ssrn.4330381 ↗.

Google Scholar ↗

Hörcher and Tirachini, 2021 D. Hörcher, A. Tirachini

A review of public transport economics

Econ. Transp., 25 (2021), Article 100196

View PDF View article View in Scopus ↗ Google Scholar ↗

Jørgensen et al., 2010 F. Jørgensen, T.A. Mathisen, G. Solvoll

Hurtigbåttilbudet i Nordland: Verdsetting og Samfunnsøkonomisk Lønnsomhet (in Norwegian)

Handelshøgskolen i Bodø, Bodø (2010)

SIB-rapport 7/2010

Google Scholar ↗

Kamen and Barry, 2011 P. Kamen, C.D. Barry

Urban passenger-only ferry systems: issues, opportunities and technologies

In

Sustainability in the Maritime Industry: A Collection of Relevant Papers, 8, Society of Naval Architects and Marine Engineers (2011), pp. 67-77

Google Scholar ↗

Klier and Haase, 2015 M.J. Klier, K. Haase

Urban public transit network optimization with flexible demand

OR Spectr., 37 (2015), pp. 195-215

CrossRef ↗ View in Scopus ↗ Google Scholar ↗

Lai and Lo, 2004 M.F. Lai, H.K. Lo

Ferry service network design: optimal fleet size, routing, and scheduling

Transp. Res. Part A Policy Pract., 38 (2004), pp. 305-328

View PDF View article View in Scopus ↗ Google Scholar ↗

Mohring, 1972 H. Mohring

Optimization and scale economies in urban bus transportation

Am. Econ. Rev., 62 (1972), pp. 591-604

Google Scholar ↗

Mojarrad et al., 2023 M. Mojarrad, M. Zadeh, K.L. Rødseth

Techno-economic modeling of zero-emission marine transport with hydrogen fuel and superconducting propulsion system: case study of a passenger ferry

Int. J. Hydrog. Energy (2023), 10.1016/j.ijhydene.2023.03.438 ↗

In press

Google Scholar ↗

Norwegian Environment Agency 2020 Norwegian Environment Agency

Klimakur 2030 (in Norwegian)

Norwegian Environment Agency, Oslo (2020)

M-1625

Google Scholar ↗

Paneque et al., 2021 M.P. Paneque, M. Bierlaire, B. Gendron, S.S. Azadeh

Integrating advanced discrete choice models in mixed integer linear optimization

Transp. Res. Part B Methodol., 146 (2021), pp. 26-49

Google Scholar ↗

Rinaldi et al., 2018 M. Rinaldi, F. Parisi, G. Laskaris, A. D'Ariano, F. Viti

Optimal dispatching of electric and hybrid buses subject to scheduling and charging constraints

Proceedings of the IEEE Conference on Intelligent Transportation Systems, ITSC (2018)

2018-November, 41–46

Google Scholar ↗

Ritari et al., 2021 A. Ritari, K. Spoof-Tuomi, J. Huotari, S. Niemi, K. Tammi

Emission abatement technology selection, routing and speed optimization of hybrid ships

J. Mar. Sci. Eng., 9 (2021), p. 944

CrossRef ↗ View in Scopus ↗ Google Scholar ↗

Rødseth et al., 2019 K.L. Rødseth, P.B. Wangsness, K. Veisten, R. Elvik, A.K. Høye, R. Klæboe, H. Thune-Larsen, L. Fridstrøm, E. Lindstad, A. Rialland, K. Odolinski, J.E. Nilsson

Eksterne Kostnader Ved Transport i Norge: Estimater av Marginale Skadekostnader for Person- og Godstransport (in Norwegian)

Transportøkonomisk Institutt, Oslo (2019)

TØI report 1704/2019

Google Scholar ↗

Rødseth et al., 2022 K.L. Rødseth, B. Dong, S. Jakobsen, J. Danebergs

Revidert modell til beregning av ferjekriteriet i inntektssystemet for fylkeskommunene

TØI-report 1914/2022, Institute of Transport Economics, Oslo. (in Norwegian) (2022)

Google Scholar ↗

Rogge et al., 2018 M. Rogge, E. van der Hurk, A. Larsen, D.U. Sauer
Electric bus fleet size and mix problem with optimization of charging infrastructure
Appl. Energy, 211 (2018), pp. 282-295
View PDF View article View in Scopus Google Scholar

Ruter 2020 Ruter
Hurtigbåt 2024
Kartlegging av Muligheter og Konsekvenser (in Norwegian), Ruter, Oslo (2020)
Google Scholar

Shang et al., 2019 H. Shang, Y. Liu, H. Huang, R. Guo
Vehicle scheduling optimization considering the passenger waiting cost
J. Adv. Transp. (2019), 10.1155/2019/4212631
Article ID 4212631
Google Scholar

Shang et al., 2023 H. Shang, Y. Liu, W. Wu, F. Zhao
Multi-depot vehicle scheduling with multiple vehicle types on overlapped bus routes
Expert Syst. Appl., 228 (2023), Article 120352
View PDF View article View in Scopus Google Scholar

Soehodo and Koshi, 1999 S. Soehodo, M. Koshi
Design of public transit network in urban area with elastic demand
J. Adv. Transp., 33 (1999), pp. 335-369
CrossRef View in Scopus Google Scholar

Sundvor et al., 2021 I. Sundvor, R.J. Thorne, J. Danebergs, Aarskog, C. Weber
Estimating the replacement potential of Norwegian high-speed passenger vessels with zero-emission solutions
Transp. Res. Part D Transp. Environ., 99 (2021), Article 103019
View PDF View article View in Scopus Google Scholar

Tveter et al., 2020 E. Tveter, K.L. Rødseth, J. Rødal, K.L. Hoff, H. Thune-Larsen
Forslag Til Nye Kriterier for Båter i Inntektssystemet for Fylkeskommunene (in Norwegian)
Møreforskning Molde, Molde (2020)
Report no. 2003
Google Scholar

Villa et al., 2020 D. Villa, A. Montoya, A.M. Herrera
The electric riverboat charging station location problem
J. Adv. Transp., 2020 (2020), Article 6527924
View in Scopus Google Scholar

Wangsness et al., 2020 P.B. Wangsness, S. Proost, K.L. Rødseth

Vehicle choices and urban transport externalities: are Norwegian policy makers getting it right?
Transp. Res. Part D Transp. Environ., 86 (2020), Article 102384
View PDF View article View in Scopus Google Scholar

Wangsness et al., 2021 P.B. Wangsness, S. Proost, K.L. Rødseth
Optimal policies for electromobility: joint assessment og transport and electricity distribution costs in Norway
Util. Policy, 72 (2021), Article 101247
View PDF View article View in Scopus Google Scholar

Wardman et al., 2016 M. Wardman, V. Phani, K. Chintakayala, G. de Jong
Values of travel time in Europe: review and meta-analysis
Transp. Res. Part A Policy Pract., 94 (2016), pp. 93-111
View PDF View article View in Scopus Google Scholar

Zhang et al., 2021 L. Zhang, Z. Zeng, K. Gao
Optimal design of mixed charging station for electric transit with joint consideration of normal charging and fast charging
Smart Innov. Syst. Technol., 231 (2021), pp. 85-94
View in Scopus Google Scholar

Cited by (0)

1 See https://www.tilnull.no/ferger (in Norwegian; accessed 05.12.2022).

2 An own-price elasticity quantifies the percentage change in transport demand that stems from a one percent increase in the price of transport. The latter is defined in terms of generalized costs of travel and encompasses fares and costs from waiting and transit times.

RELX™